Photoproduction of Λ^* Resonances at CLAS

CLAS Collaboration Meeting
November 12, 2020

Utsav Shrestha, Ken Hicks & Chaden Djalali
Ohio University

Supported in part by a grant from the NSF.

Introduction

The Quark Model

J^P	$(D, L_N^P)\, S$	Octet members				Singlets
$1/2^+$	$(56,0_0^+)$ $1/2$	$N(939)$	$\Lambda(1116)$	$\Sigma(1193)$	$\Xi(1318)$	
$1/2^+$	$(56,0_2^+)$ $1/2$	$N(1440)$	$\Lambda(1600)$	$\Sigma(1660)$	$\Xi(1690)^\dagger$	
$1/2^-$	$(70,1_1^-)$ $1/2$	$N(1535)$	$\boxed{\Lambda(1670)}$	$\Sigma(1620)$	$\Xi(?)$	$\boxed{\Lambda(1405)}$
				$\Sigma(1560)^\dagger$		
$3/2^-$	$(70,1_1^-)$ $1/2$	$N(1520)$	$\boxed{\Lambda(1690)}$	$\Sigma(1670)$	$\Xi(1820)$	$\boxed{\Lambda(1520)}$
$1/2^-$	$(70,1_1^-)$ $3/2$	$N(1650)$	$\Lambda(1800)$	$\Sigma(1750)$	$\Xi(?)$	
				$\Sigma(1620)^\dagger$		
$3/2^-$	$(70,1_1^-)$ $3/2$	$N(1700)$	$\Lambda(?)$	$\Sigma(1940)^\dagger$	$\Xi(?)$	
$5/2^-$	$(70,1_1^-)$ $3/2$	$N(1675)$	$\Lambda(1830)$	$\Sigma(1775)$	$\Xi(1950)^\dagger$	
$1/2^+$	$(70,0_2^+)$ $1/2$	$N(1710)$	$\Lambda(1810)$	$\Sigma(1880)$	$\Xi(?)$	$\Lambda(1810)^\dagger$
$3/2^+$	$(56,2_2^+)$ $1/2$	$N(1720)$	$\Lambda(1890)$	$\Sigma(?)$	$\Xi(?)$	
$5/2^+$	$(56,2_2^+)$ $1/2$	$N(1680)$	$\Lambda(1820)$	$\Sigma(1915)$	$\Xi(2030)$	
$7/2^-$	$(70,3_3^-)$ $1/2$	$N(2190)$	$\Lambda(?)$	$\Sigma(?)$	$\Xi(?)$	$\Lambda(2100)$
$9/2^-$	$(70,3_3^-)$ $3/2$	$N(2250)$	$\Lambda(?)$	$\Sigma(?)$	$\Xi(?)$	
$9/2^+$	$(56,4_4^+)$ $1/2$	$N(2220)$	$\Lambda(2350)$	$\Sigma(?)$	$\Xi(?)$	

Lattice QCD Calculations

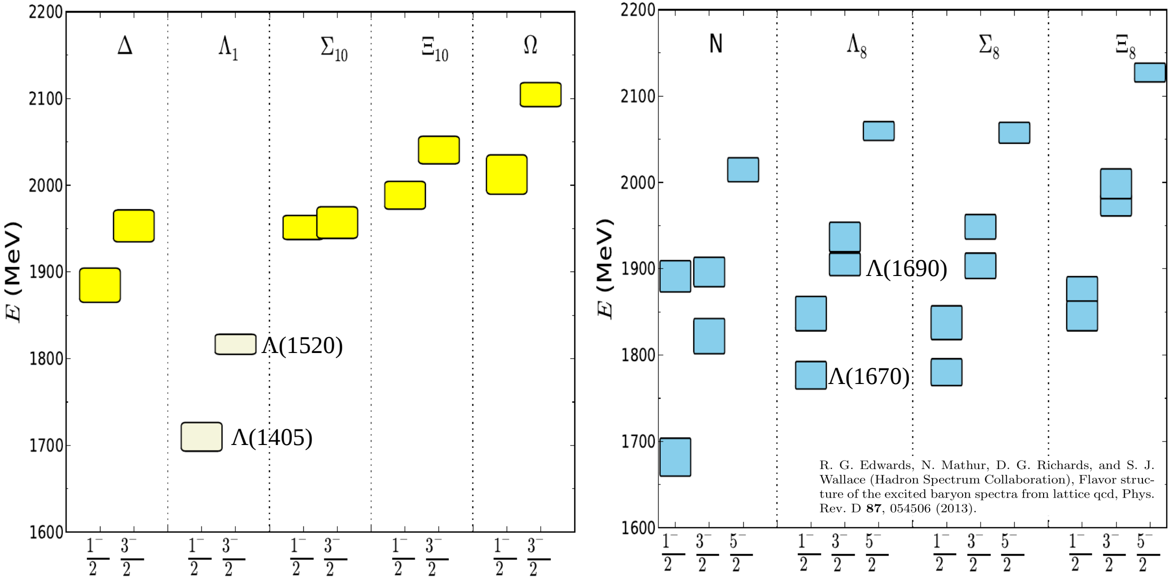

R. G. Edwards, N. Mathur, D. G. Richards, and S. J. Wallace (Hadron Spectrum Collaboration), Flavor structure of the excited baryon spectra from lattice qcd, Phys. Rev. D **87**, 054506 (2013).

The Particle Data Group Summary

Particle	J^P	PDG rating	Status as seen in $N\overline{K}$	$\Lambda\pi$	$\Sigma\pi$	Other Channels
$\Lambda(1405)$	1/2-	****	****		****	
$\Lambda(1520)$	3/2-	****	****	Forbidden	****	$\Lambda\pi\pi$, $\Lambda\gamma$
$\Lambda(1670)$	1/2-	****	****		****	$\Lambda\eta$
$\Lambda(1690)$	3/2-	****	****		****	$\Lambda\pi\pi$, $\Sigma\pi\pi$

Phase at Resonances in $\Sigma\pi$ Channel

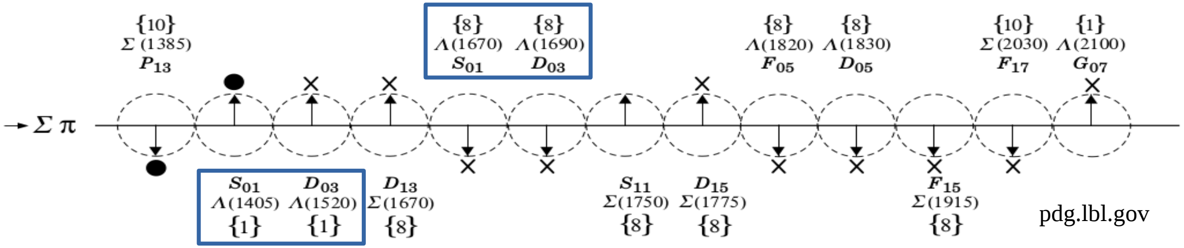

The Reaction

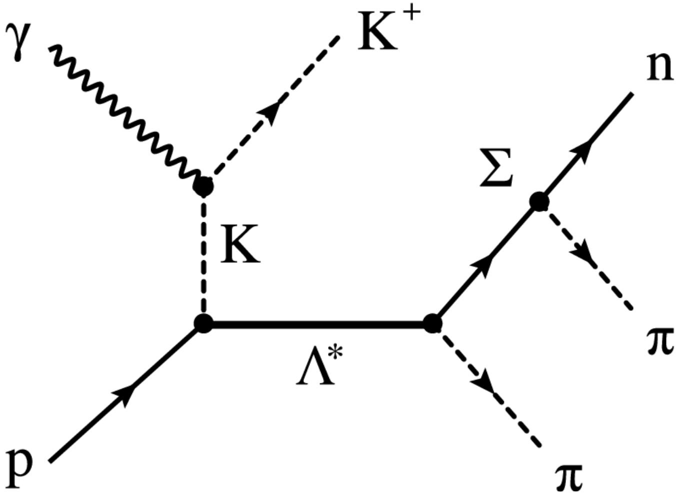

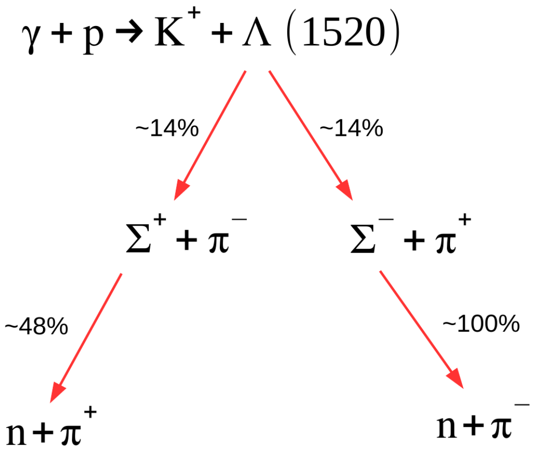

$$\gamma p \to K^+\Lambda(1520) \to K^+\Sigma^\pm\pi^\mp$$

$$\Lambda(1520) \to \Sigma^\pm\pi^\mp \to n\pi^\pm\pi^\mp$$

Data Analysis

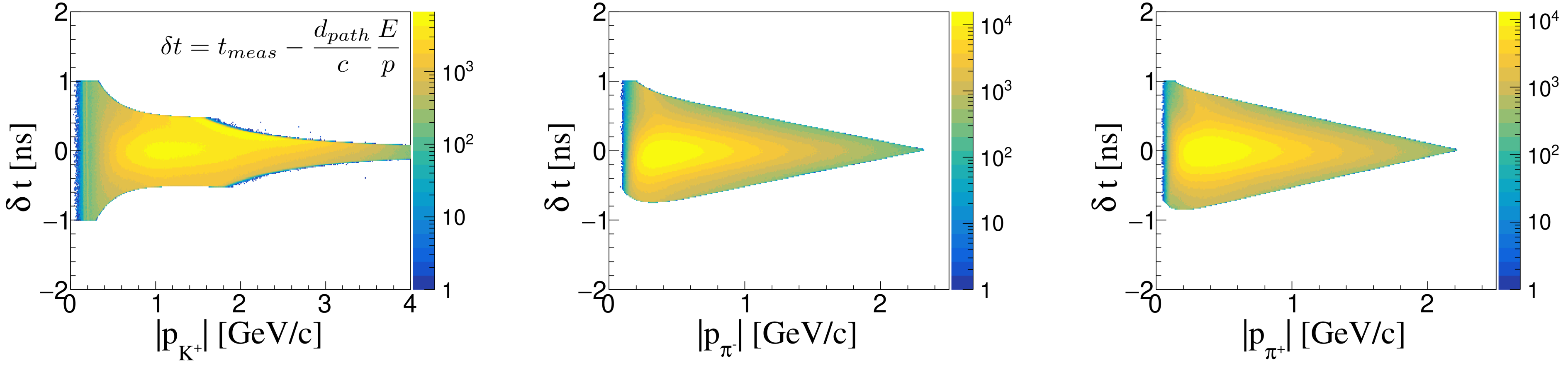

Skim
Photon Selection
$K^+\pi^+\pi^-$ PID Cut
Minimum $|p|$ cut
z-vertex cut
Nominal Fiducial Cut
SC Paddle Cut

$0.9 \leq MM(K^+\pi\pi) \leq 1.0$	Select neutron events
$0.48 \leq IM(\pi^+\pi^-) \leq 0.51$	Remove nK^0 channel
$1.15 \leq MM(K^+\pi^-) \leq 1.25$ $1.15 \leq MM(K^+\pi^+) \leq 1.25$	Select Σ^+ and Σ^- events for exclusive $\Sigma\pi$ channels
$1.44 \leq MM(K^+) \leq 1.6$	Fitting Range $\Lambda(1520)$
$2.25 \leq W \leq 3.25$ GeV $-0.9 \leq \cos\theta^{K+}_{cm} \leq 0.9$ $-2.7 \leq t \leq -0.3$	Binning Scheme

Data Analysis

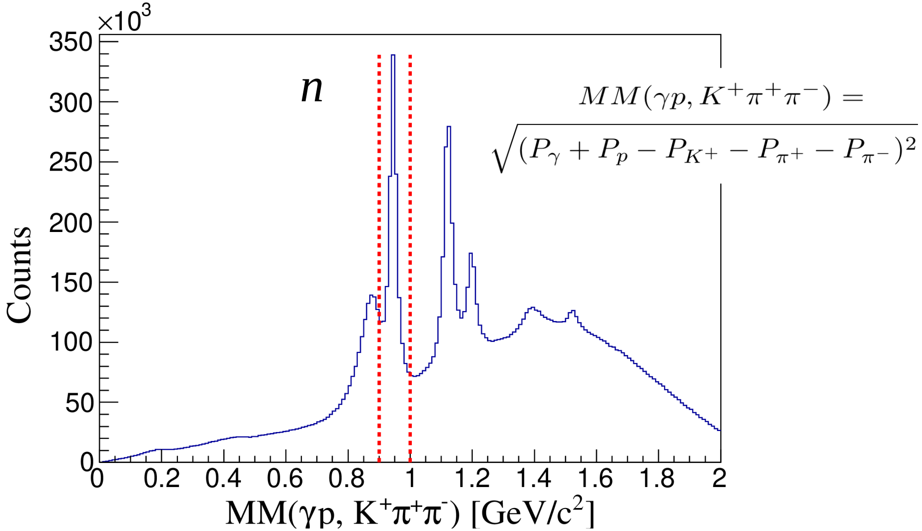

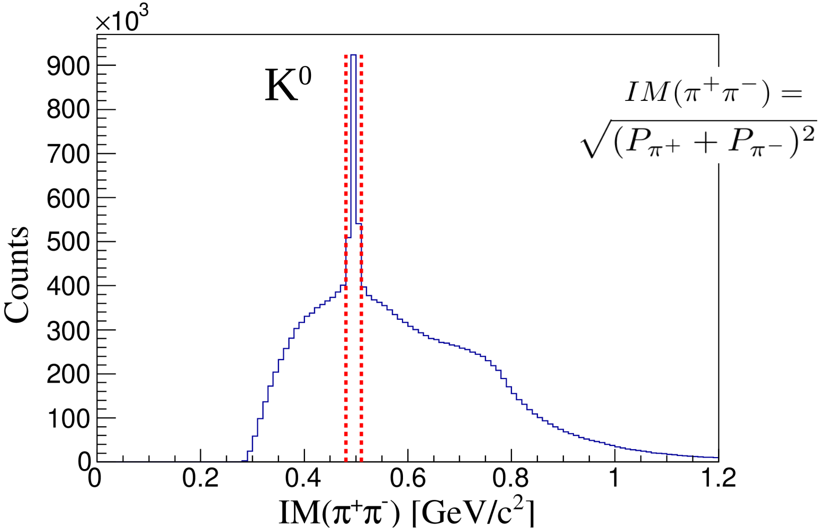

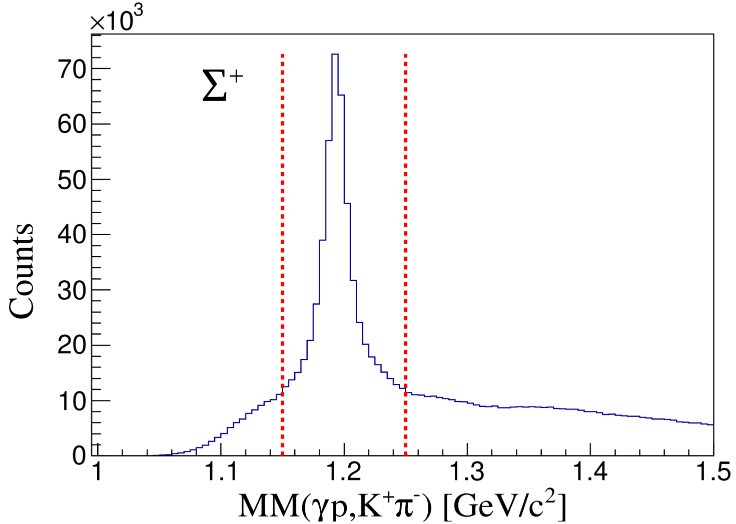

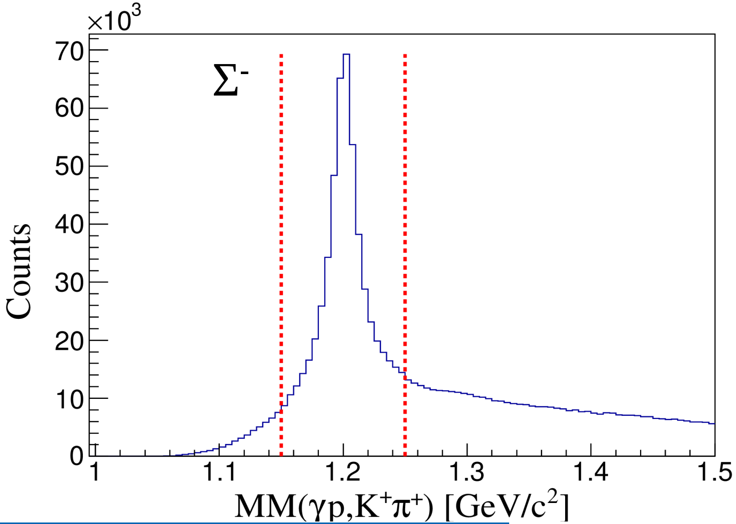

Data Analysis

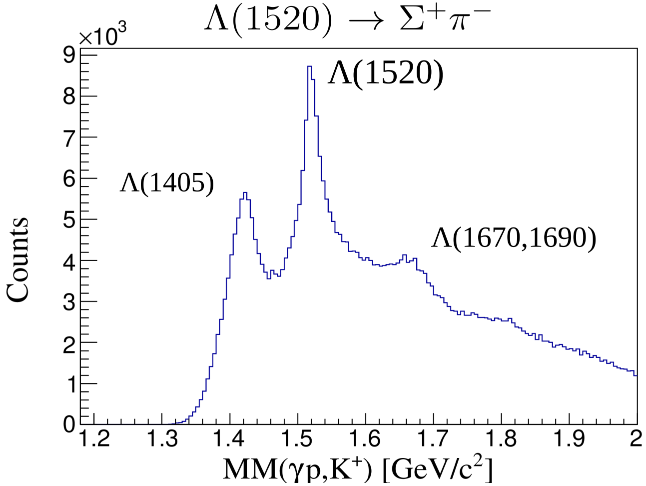

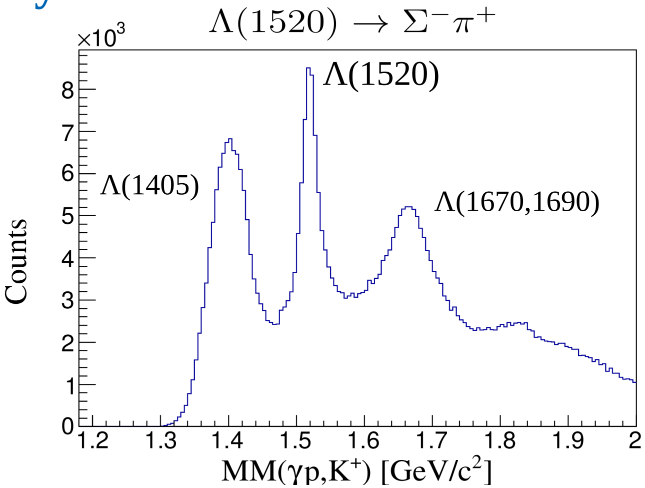

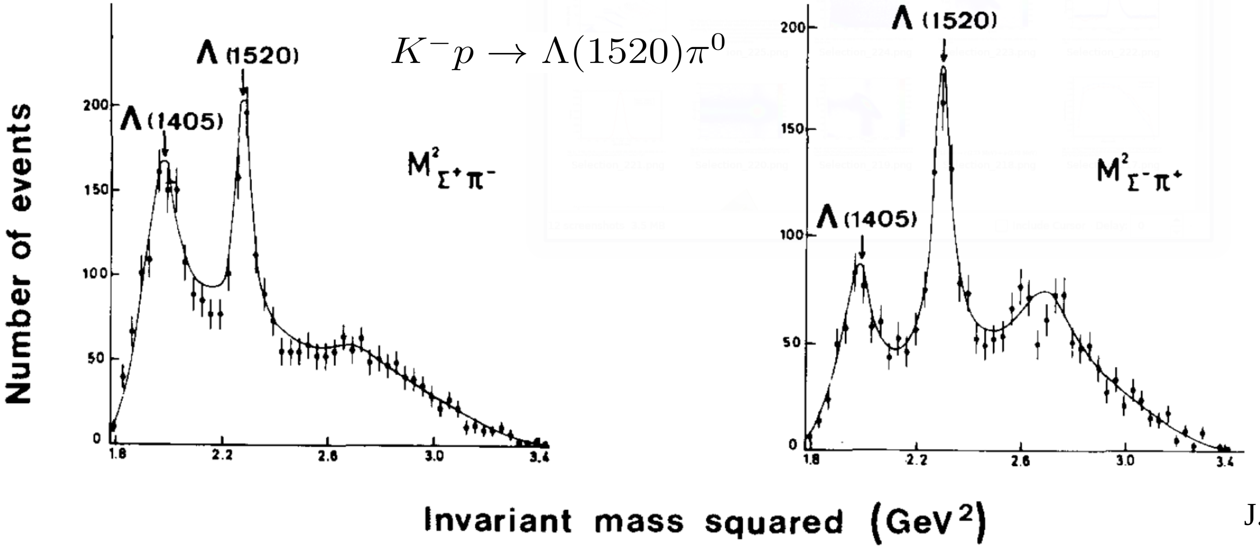

J. Griselin *et. al.*, 1975

Data Analysis

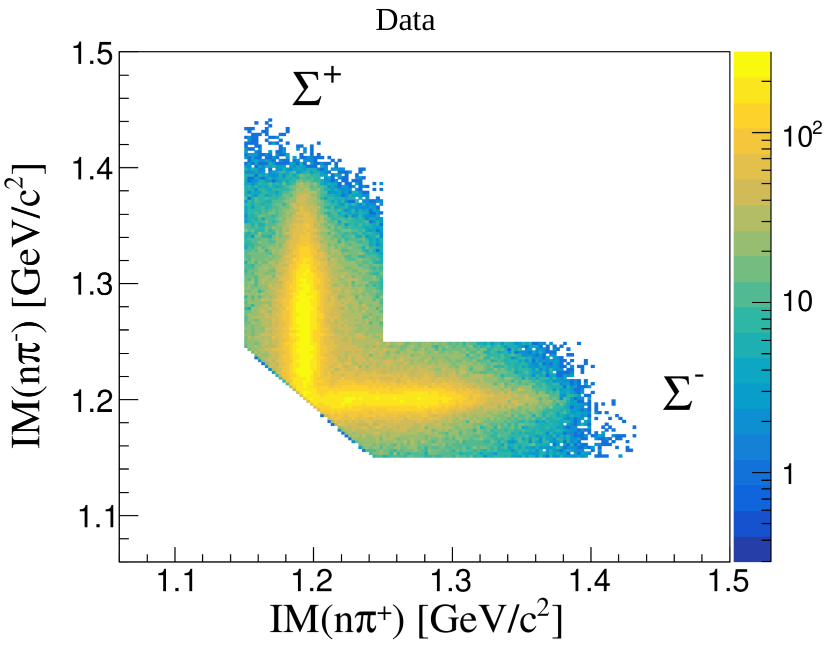

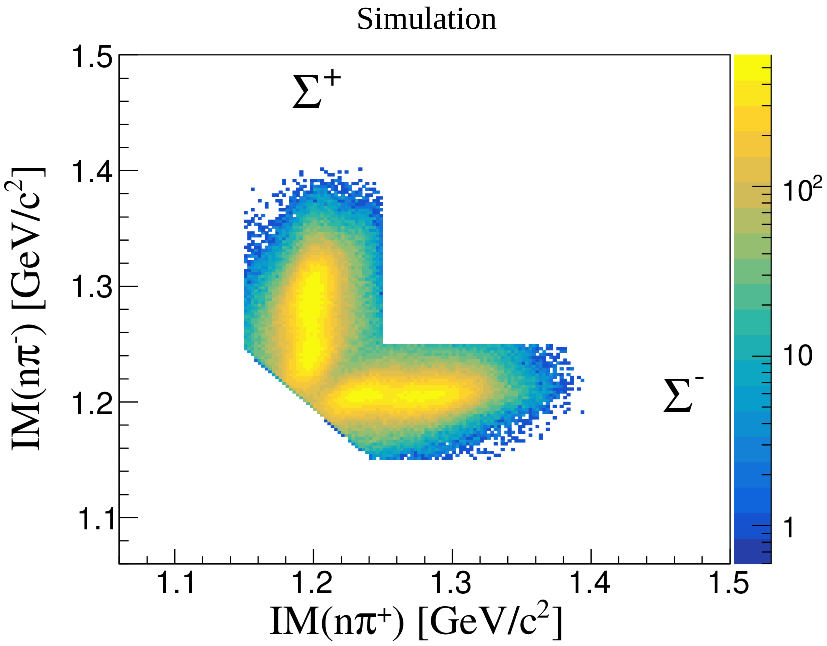

Data Analysis

Binning Scheme in W & $cos\theta^{cm}_{K+}$

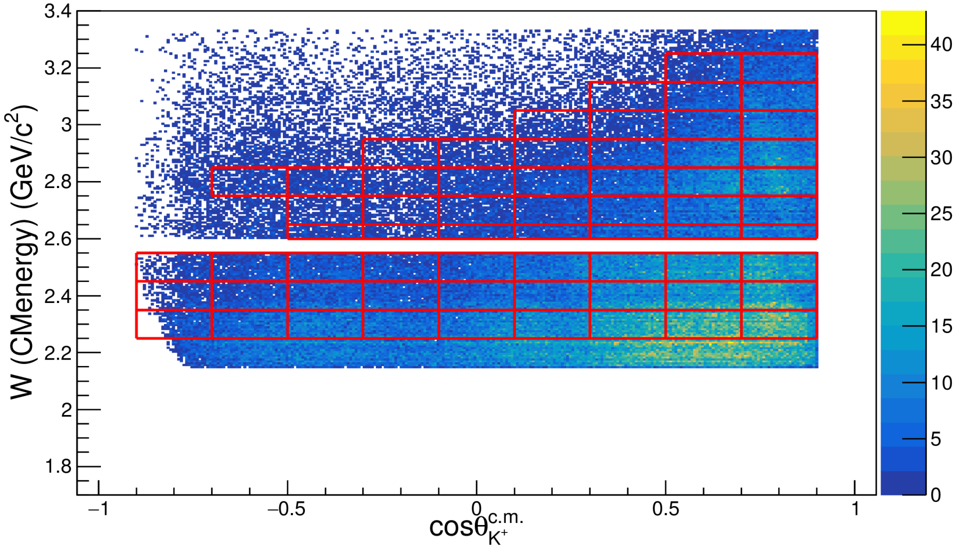

Binning Scheme in W & t

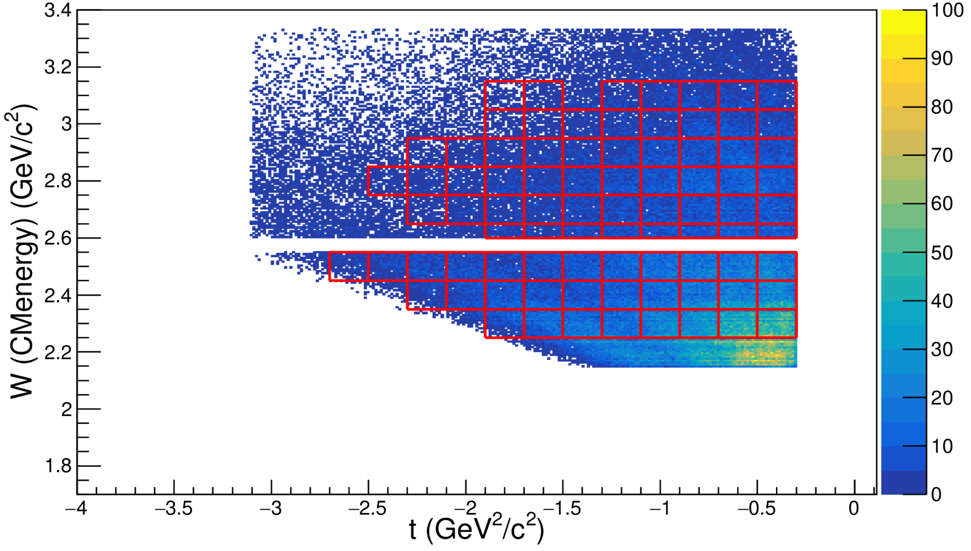

Data Analysis

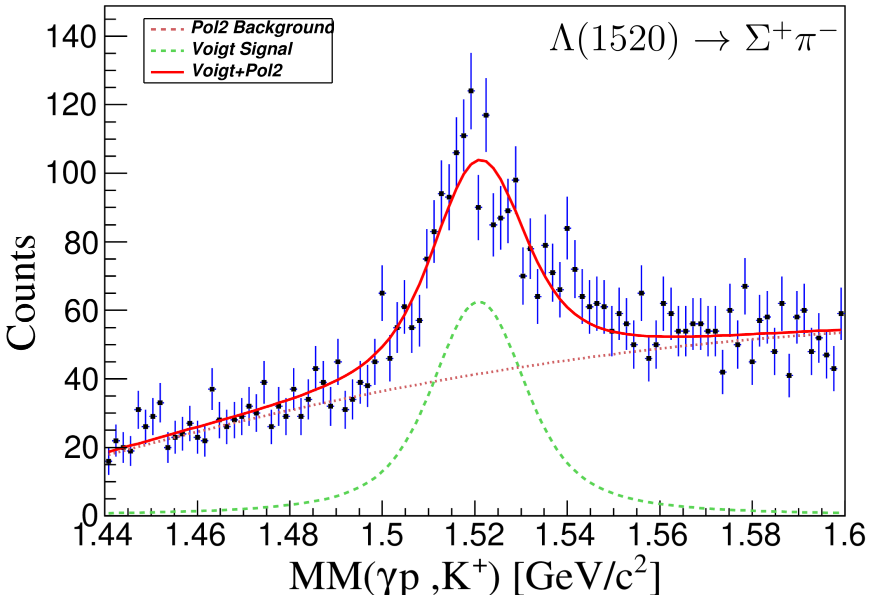

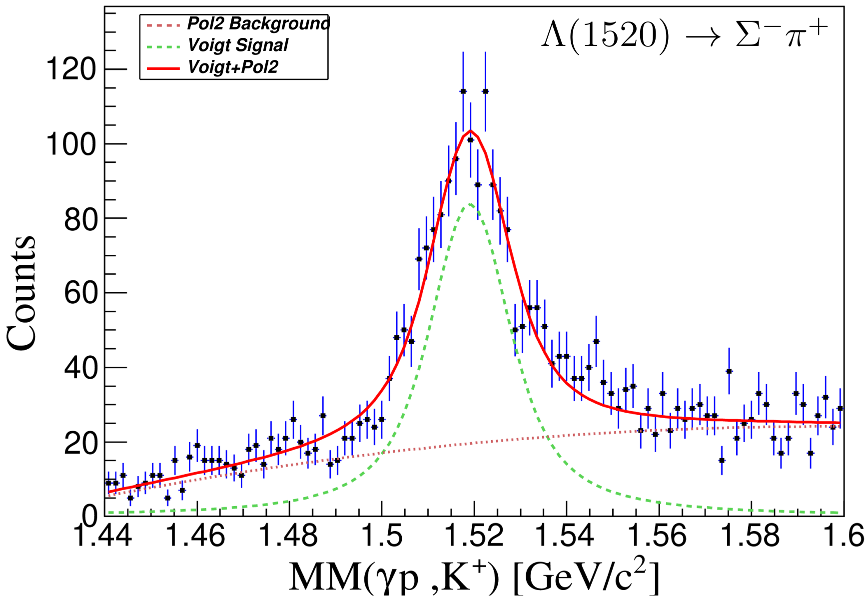

Differential Cross-sections

$$\frac{d\sigma}{d\cos\theta^{c.m.}_{K^+}} = \frac{Y(W,\cos\theta^{c.m.}_{K^+})}{\tau\Delta\cos\theta^{c.m.}_{K^+} A(W,\cos\theta^{c.m.}_{K^+})L(W)}$$

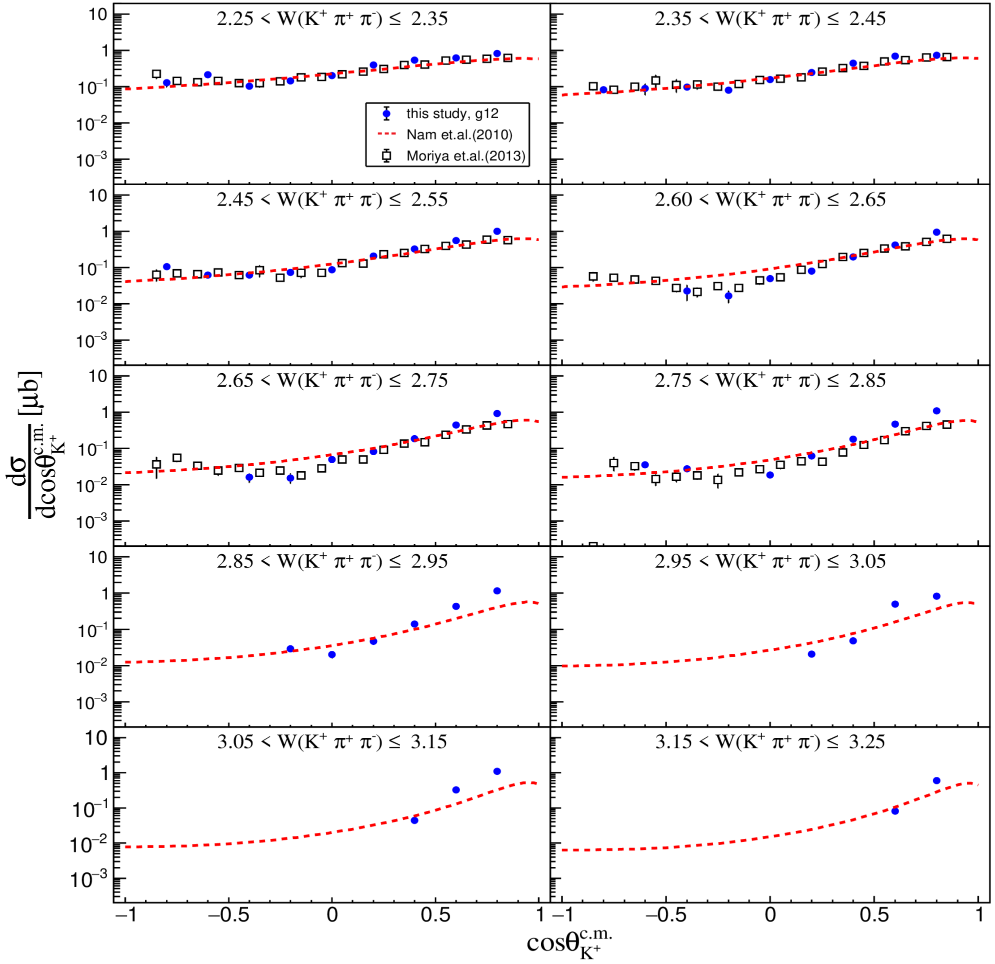

$$\frac{d\sigma}{dt} = \frac{Y(W,t)}{\tau\Delta t A(W,t)L(W)}$$

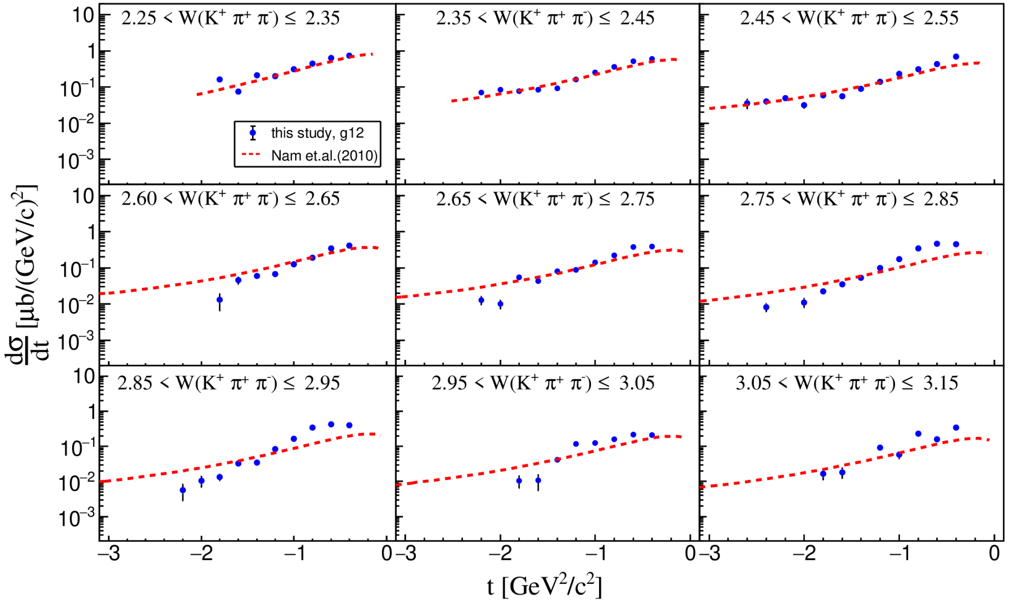

- The Λ(1520) differential cross sections are shown as a function of CM angle and invariant 4-momentum transfer *t*, and extented for higher *W*.
- The *g12* results are in good agreement with previous CLAS measurements.
- The model calculations by Nam *et. al.* (2010), shown as dashed curves, reproduce the data very well.
- Some deviations at forward angles for *W* > 2.7 GeV may need more sophisticated theoretical approaches.

Systematic Uncertainties

Source	Description	Uncertainty
t-slope dependence	b = 2.0 *vs.* b = 1.0	0.78%
Timing Cut	3σ *vs.* 2.5σ	4.11%
Minimum $\|p\|$ cut	Minimum $\|p\|$ *vs.* no cut	0.20%
z-Vertex Cut	$-110 < z < -70$ *vs.* $-108 < z < -72$	1.28%
Fiducial Cut	50%(nominal) *vs.* 100%(tight)	3.13%
Background Function	*Pol2 vs. Pol1*	2.07%
Signal Integration Range	3.0σ *vs.* 3.5σ	0.43%
Flux Consistency/Luminosity	*g12*	1.70%
Sector by Sector	*g12*	5.90%
Target	*g12*	0.50%
Total Systematic Uncertainty	Added in quadrature	8.45%

Discussion and Conclusion

- The theory calculations are the numerical results without the N^* contribution, and conserve gauge invariance.

- Theoretical study has concluded that the K^*-N-$\Lambda(1520)$ coupling must be very small to explain the data.

- Calculations with N^* show very small contribution, just above threshold, and is limited to the first W bin. Such calculations include only N^* resonances with mass below 2.2 GeV.

- The simplest theoretical model with a pseudoscalar K-meson exchange, assuming t-channel dominance, is sufficient to explain our data, without other processes like Regge, K^* and hyperon resonances. No new N^* resonances decaying into $K^+\Lambda(1520)$ final state are found.

- This theoretical model can be used to study higher N^* resonances as well.

$\Lambda(1670)$ & $\Lambda(1690)$

Particle	J^P	PDG rating	Status as seen in			
			$N\overline{K}$	$\Lambda\pi$	$\Sigma\pi$	Other Channels
$\Lambda(1405)$	1/2-	****	****	Forbidden	****	
$\Lambda(1520)$	3/2-	****	****		****	$\Lambda\pi\pi$, $\Lambda\gamma$
$\Lambda(1670)$	1/2-	****	****		****	$\Lambda\eta$
$\Lambda(1690)$	3/2-	****	****		****	$\Lambda\pi\pi$, $\Sigma\pi\pi$

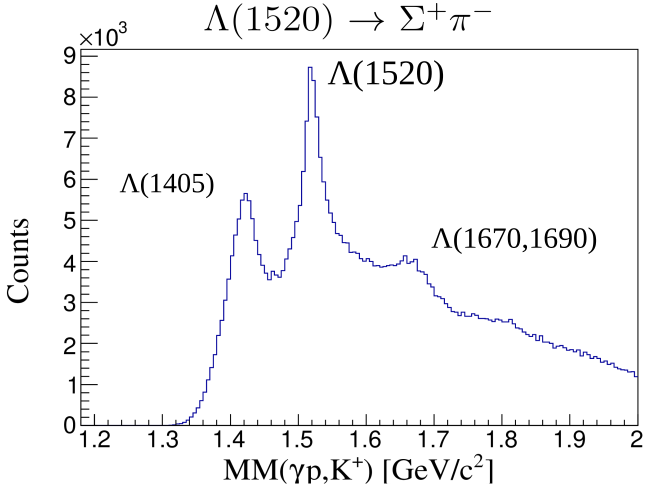

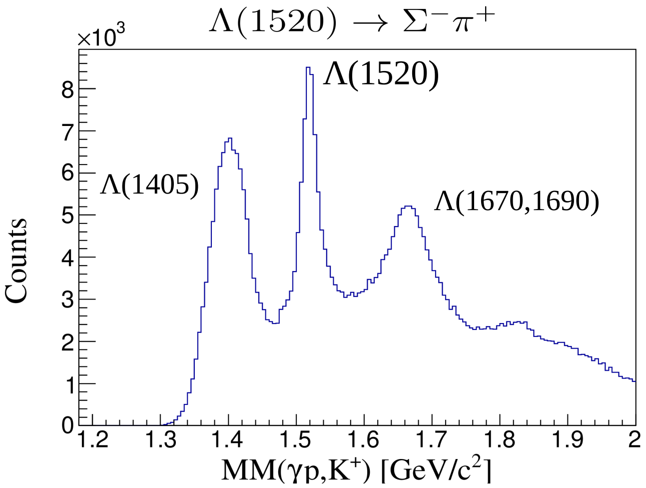

$\Lambda(1670)$ & $\Lambda(1690)$

$\Lambda^* \rightarrow \Sigma^+\pi^-$ or $\Sigma^-\pi^+$

$\langle 0\ 0 \mid 1\ {+1}\ 1\ {-1}\rangle = 1/\sqrt{3}$

$\langle 0\ 0 \mid 1\ {-1}\ 1\ {+1}\rangle = 1/\sqrt{3}$

Σ^0 coupling to the decay of $\Sigma^+\pi^-$ & $\Sigma^-\pi^+$

$\Sigma^0 \rightarrow \Sigma^+\pi^-$ or $\Sigma^-\pi^+$

$\langle 1\ 0 \mid 1\ {+1}\ 1\ {-1}\rangle = 1/\sqrt{2}$

$\langle 1\ 0 \mid 1\ {-1}\ 1\ {+1}\rangle = -1/\sqrt{2}$

$\boxed{\Sigma(1670)\ 3/2^-}$ $I(J^P) = 1(\frac{3}{2}^-)$

Mass m = 1665 to 1685 ($\approx$ 1670) MeV
Full width Γ = 40 to 80 ($\approx$ 60) MeV

Σ(1670) DECAY MODES	Fraction (Γ_i/Γ)	p (MeV/c)
$N\overline{K}$	7–13 %	414
$\Lambda\pi$	5–15 %	448
$\Sigma\pi$	30–60 %	394

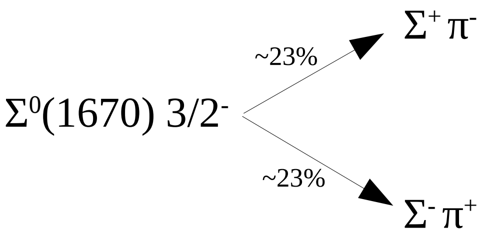

Phase at Resonances in $\Sigma\pi$ Channel

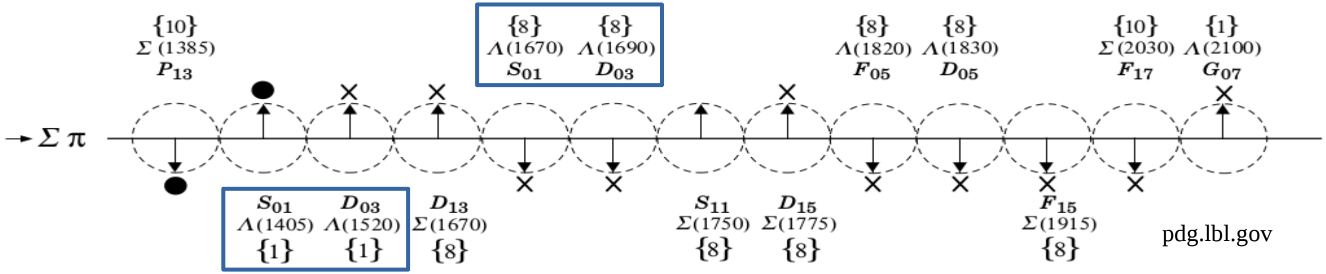

$\Lambda(1520) \rightarrow \Sigma\,\pi$

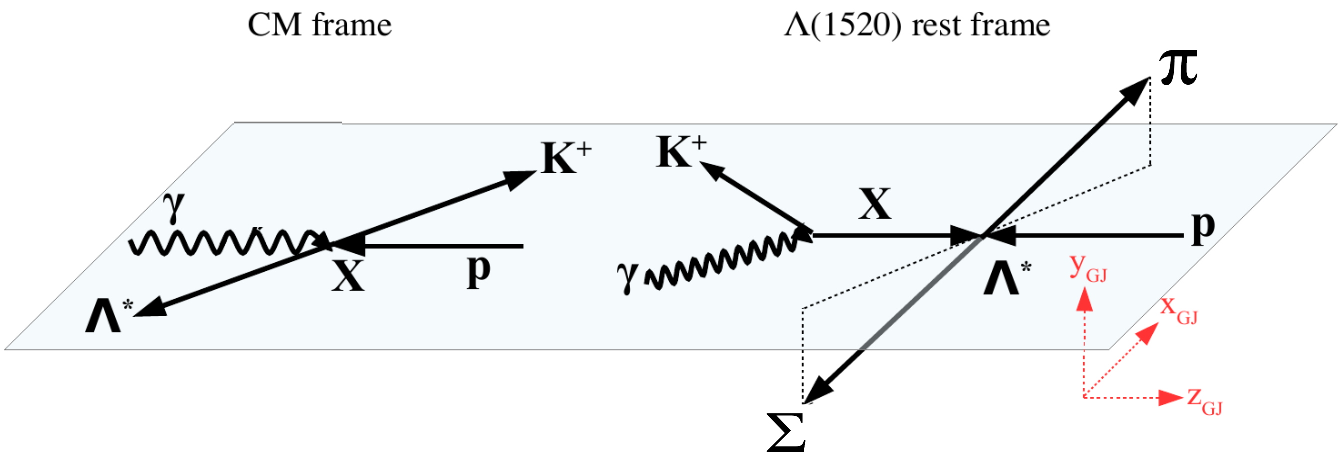

$\Lambda(1520) \rightarrow \Sigma\,\pi$

$3/2^- \rightarrow 1/2^+\,0^-$

$$I(\cos\theta,\phi)=\frac{3}{4\pi}\Big\{\varrho_{33}\sin^2\theta+\varrho_{11}\big(\tfrac{1}{3}+\cos^2\theta\big) - \frac{2}{\sqrt{3}}\mathrm{Re}\,\varrho_{31}\sin 2\theta\cos\phi-\frac{2}{\sqrt{3}}\mathrm{Re}\,\varrho_{3-1}\sin^2\theta\,\cos 2\phi\Big\}$$

Barber *et. al.*, (1980)

The Λ(1520) spin density matrix elements are connected with the angular distribution of the decay products as parameters which multiply the angular functions.

$\Lambda(1520)$ Fit with *sPlot*

- We used *brufit* framework based on *RooFit*, developed by Derek Glazier. With help from him, we were able to proceed in our analysis.

- First, the so-called *sPlot* technique is applied to separate data distributions using a discriminatory variable, MM(K^+), before actually fitting to the angular distributions of the final state.

- An event-by-event maximum likelihood fit to MM(K^+) is performed to determine the contributions from signal and background to the $\Lambda(1520)$ peak.

- An event-by-event *sWeight* is calculated for signal and background, which are then applied to the angular distributions on an event-by-event basis.

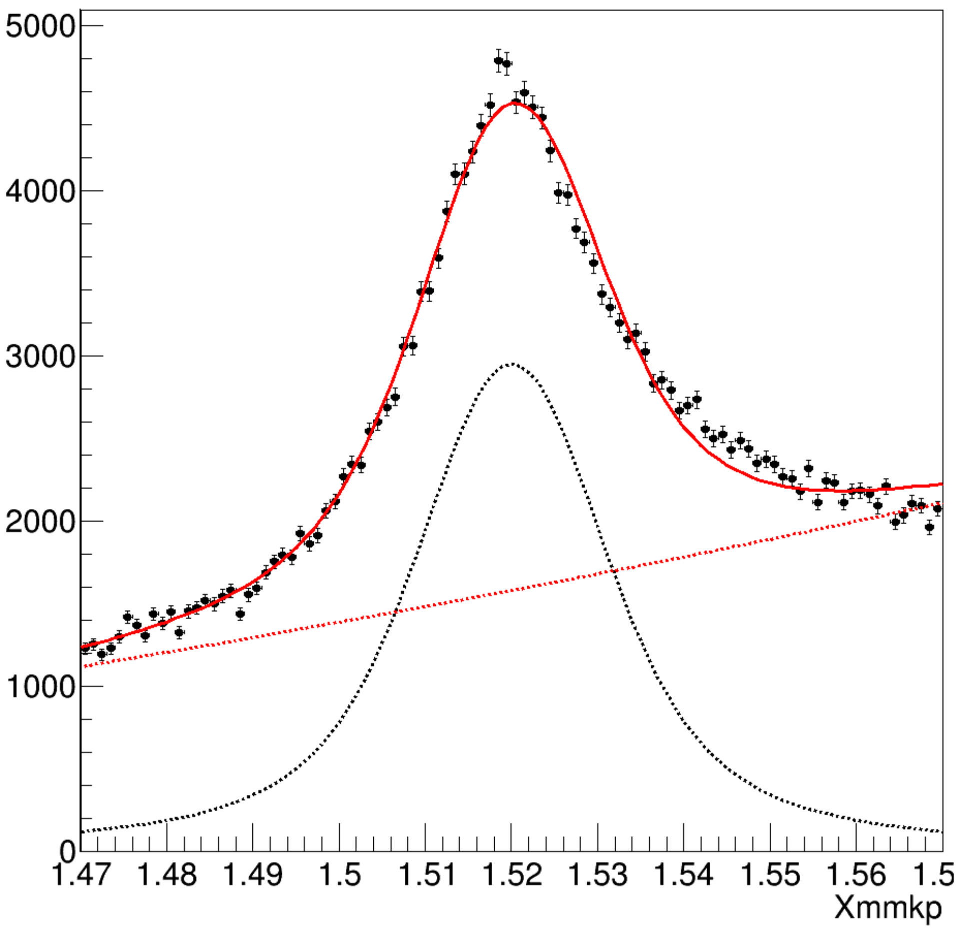

https://github.com/dglazier/brufit

Λ(1520) angular decay distributions

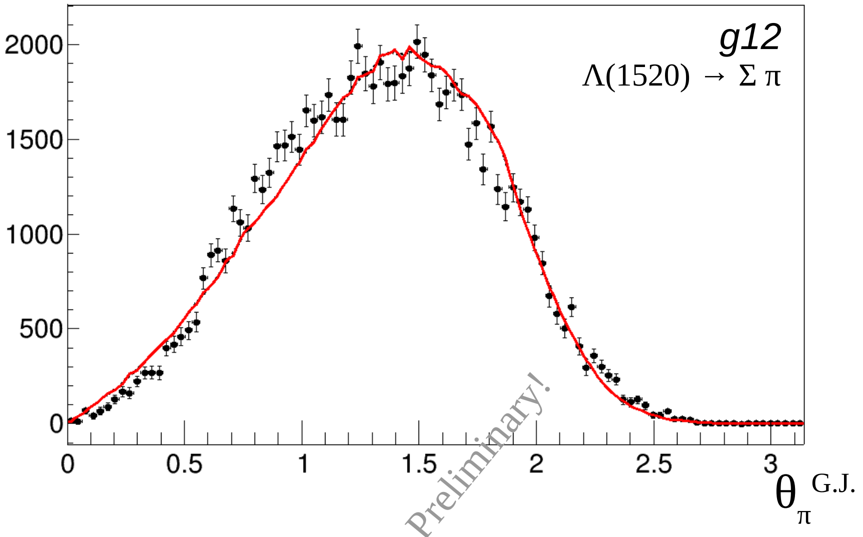

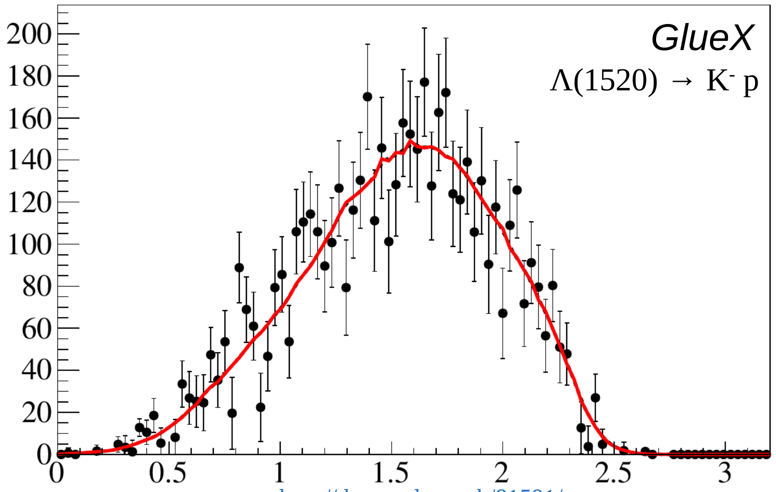

http://theses.gla.ac.uk/81591/
Pauli, Peter (2020) PhD thesis, GlueX.

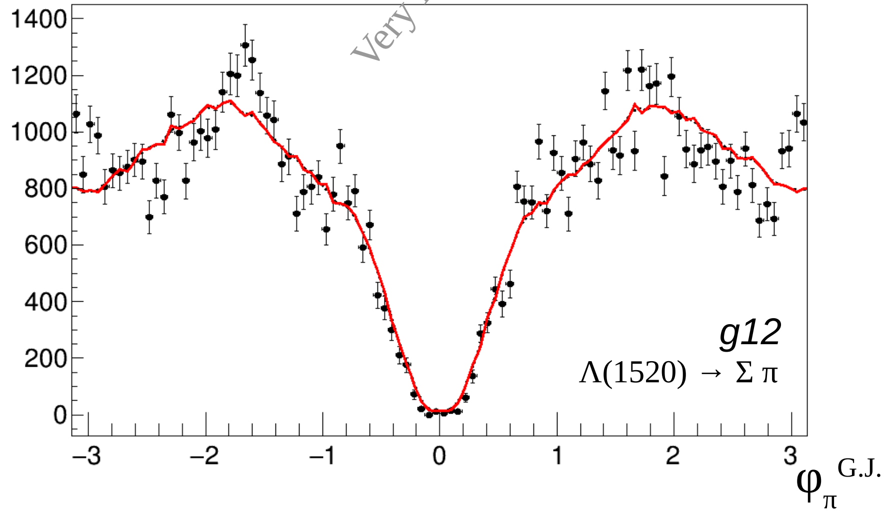

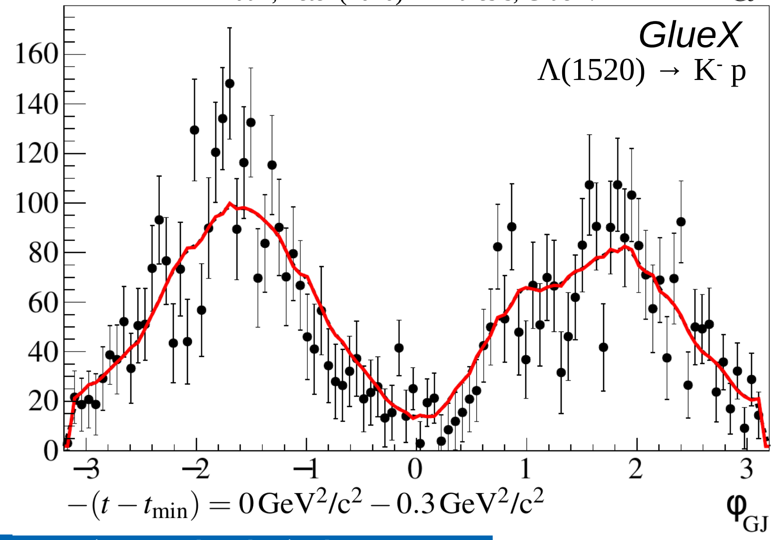

$\Lambda(1520)$ SDME

$\Lambda(1520) \to \Sigma\pi$

$\rho_{11} = 0.1755 \pm 0.0050$

$\rho_{31} = 0.10321 \pm 0.0045$

$\rho_{3-1} = 0.0615 \pm 0.0043$

Very Preliminary!

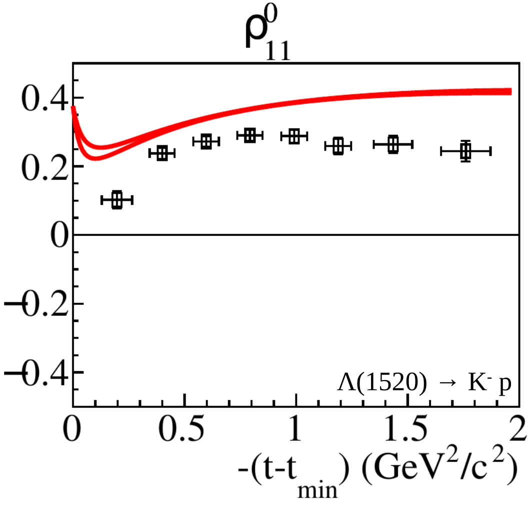

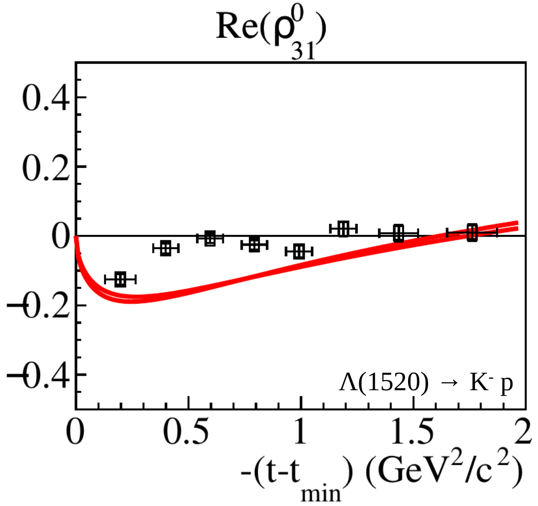

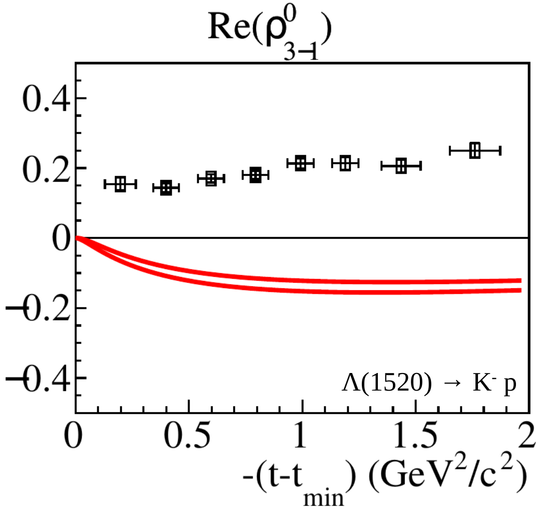

http://theses.gla.ac.uk/81591/
Pauli, Peter (2020) PhD thesis, GlueX.

B. G. Yu and K. J. Kong. Photoproduction of $\gamma p \to K + \Lambda^*(1520)$ and decay of $\Lambda^*(1520) \to K^- p$ in the Reggeized framework. *Physical Review C*, 96(2):025208, 2017.

Outlook

- The higher mass resonance region has peak contributions from $\Lambda(1670)1/2^{-}$ & $\Lambda(1690)3/2^{-}$.
- $\Sigma(1670)3/2^{-}$ peak interferes destructively for $\Sigma^{+}\pi^{-}$ channel and constructively for $\Sigma^{-}\pi^{+}$ channel.
- Our goal is to somehow use the decay angular distributions of the resonances to separate the $J^P = 1/2^{-}$ and $J^P = 3/2^{-}$.
- Using the spin density matrix elements, we want to fit the decay angular distribution for a resonance and select out the events corresponding to different $J^P = 1/2^{-} \sim \Lambda(1670)$ and $J^P = 3/2^{-} \sim \Lambda(1690)$.

Thank You!

Extras

CLAS @ JLab

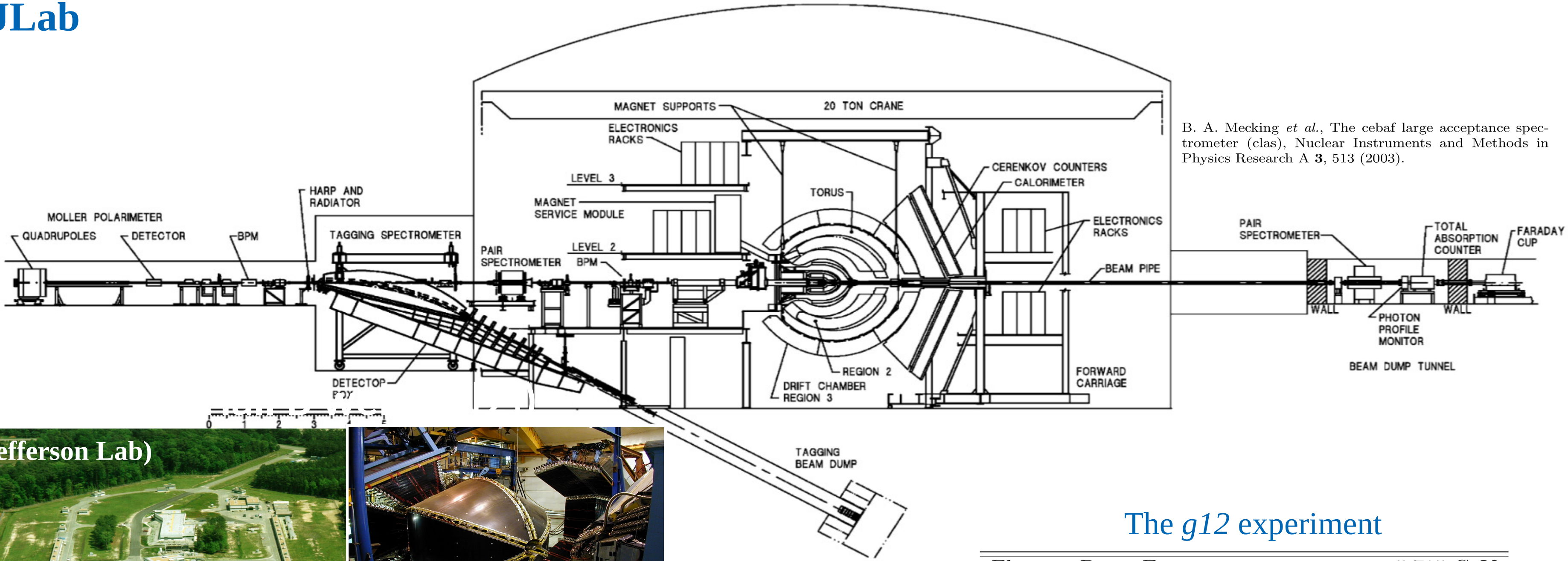

B. A. Mecking *et al.*, The cebaf large acceptance spectrometer (clas), Nuclear Instruments and Methods in Physics Research A **3**, 513 (2003).

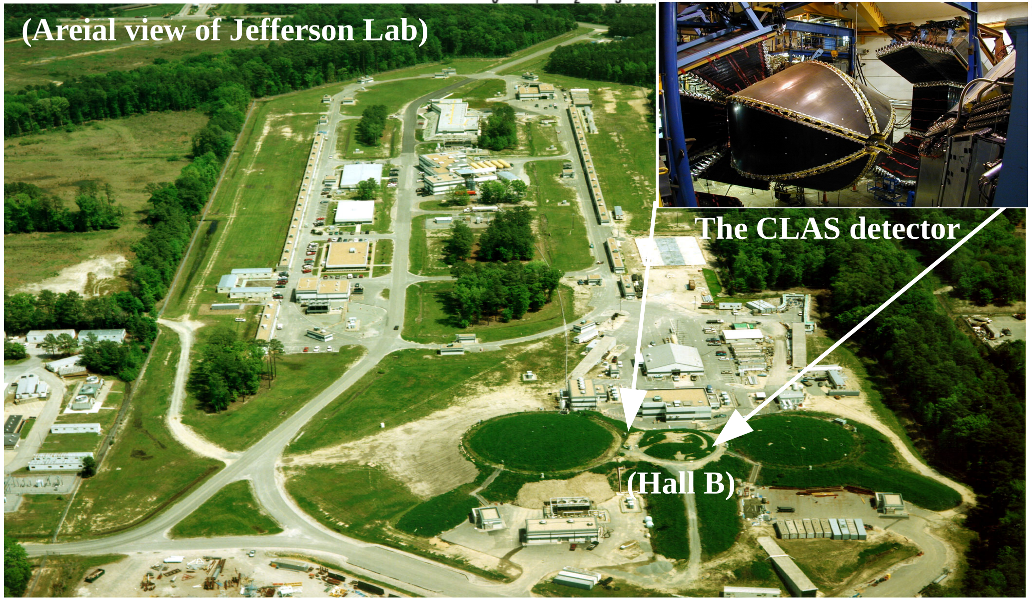

The *g12* experiment

Electron Beam Energy	5.715 GeV
Beam Polarization	Circular
e^- Current	60–65 nA
Tagger Range	20% - 95% of e^- energy
Tagger Trigger Range	3.6 - 5.441 GeV
Torus Magnet	$\frac{1}{2}B_{max}(1930A)$
Target Length	40 cm
Target Center (z location)	-90 cm
Target Material	LH_2
Target Polarization	None
Start Counter Offset	0 cm
Radiator Thickness	10^{-4} radiation lengths
Collimator Radius	6.4 mm

$K^{*0} \rightarrow K^+ \pi^-$ Backgound

Model prediction showing the difference in K^{*0} background contributions to the decay of Λ^* into two channels $\Sigma^+ \pi^-$ (red) and $\Sigma^- \pi^+$ (blue).

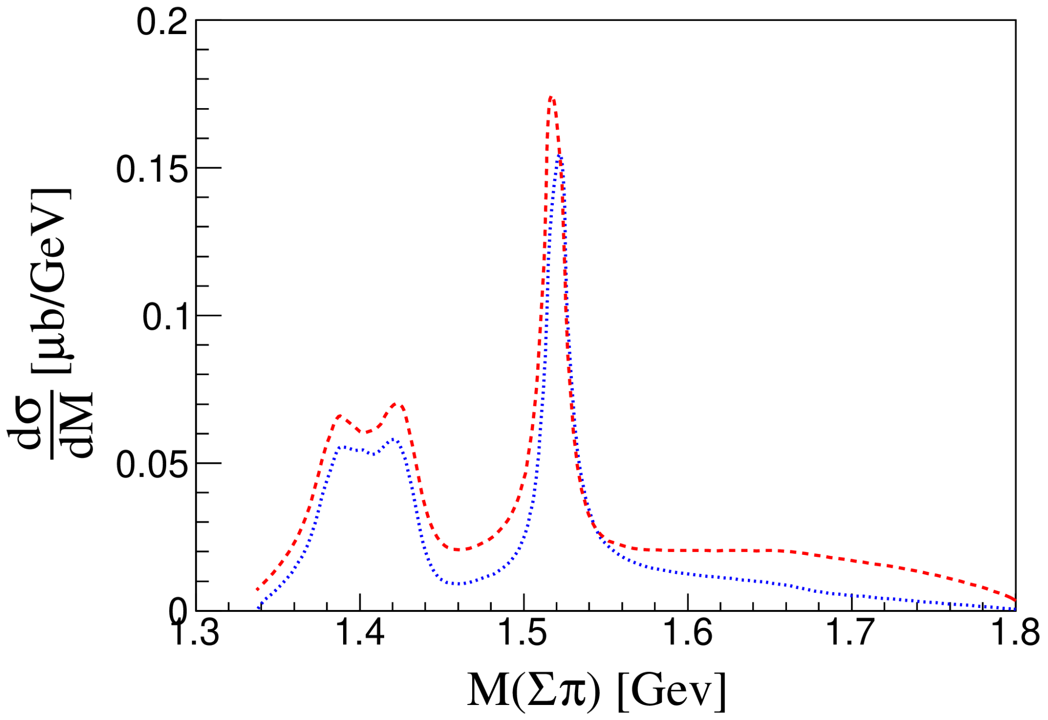

$\Lambda\,(1670,1690) \rightarrow \Sigma^{+} + \pi^{-}$

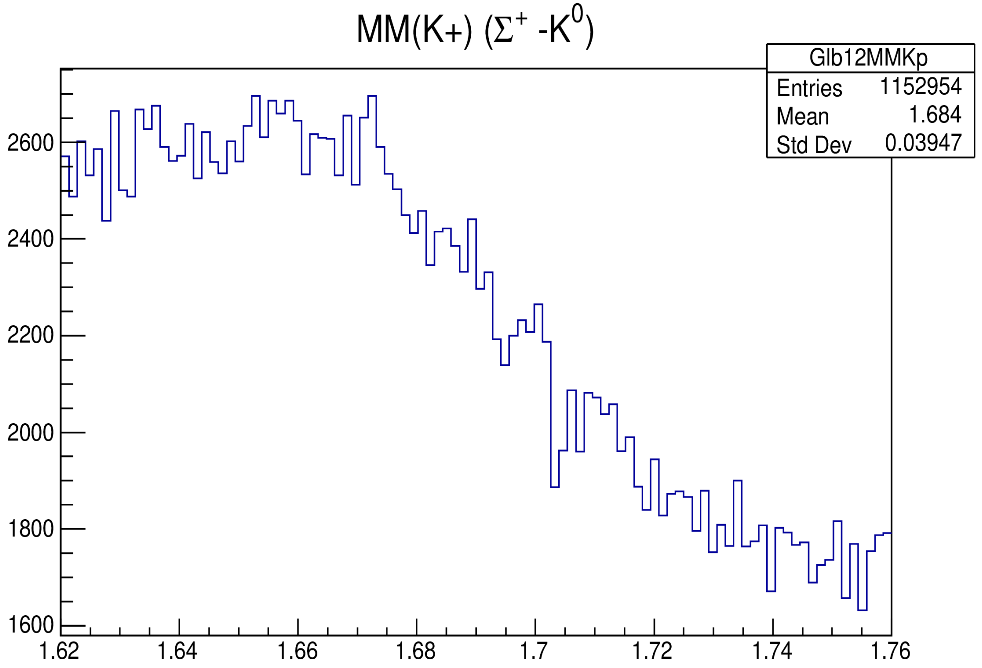

$\Lambda\,(1670,1690) \rightarrow \Sigma^{-} + \pi^{+}$

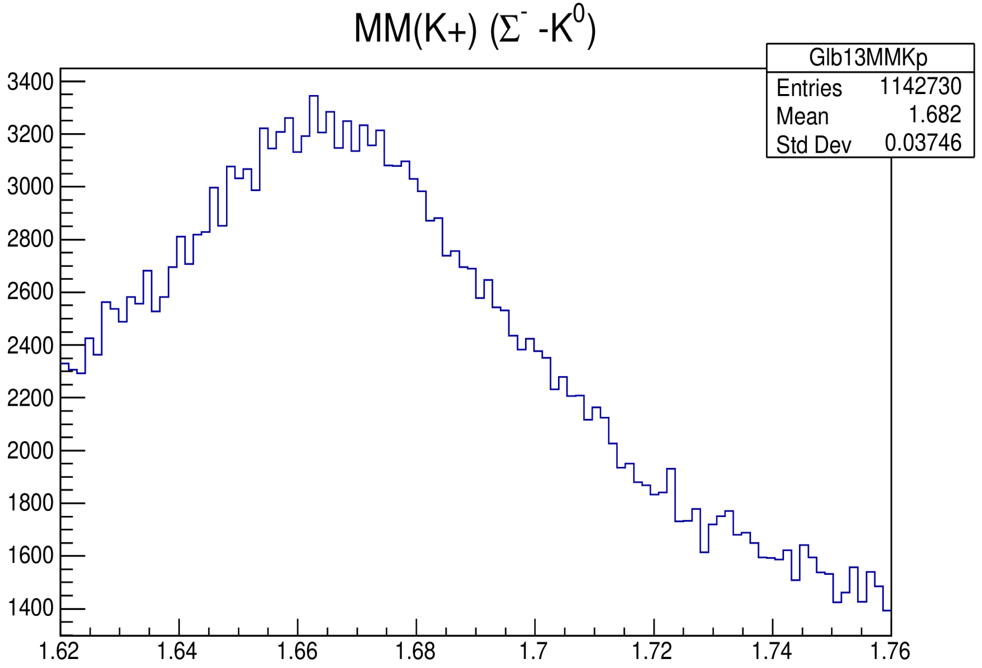

Trigger Correction “new”

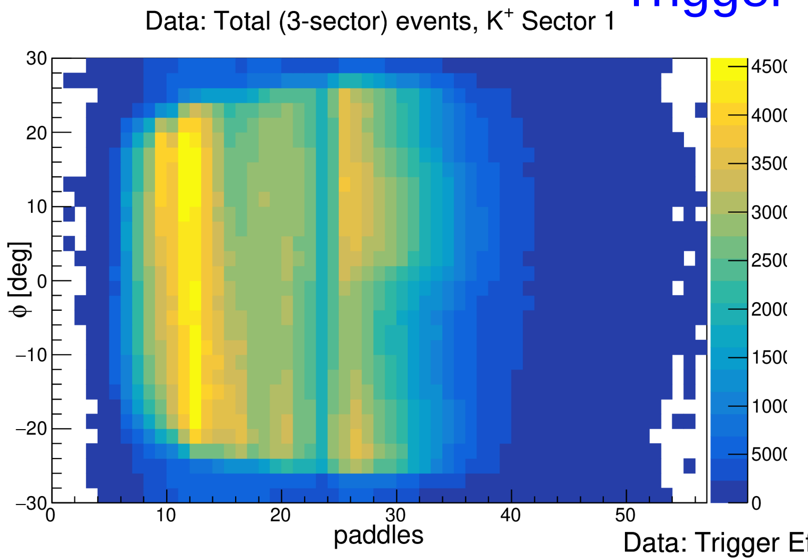

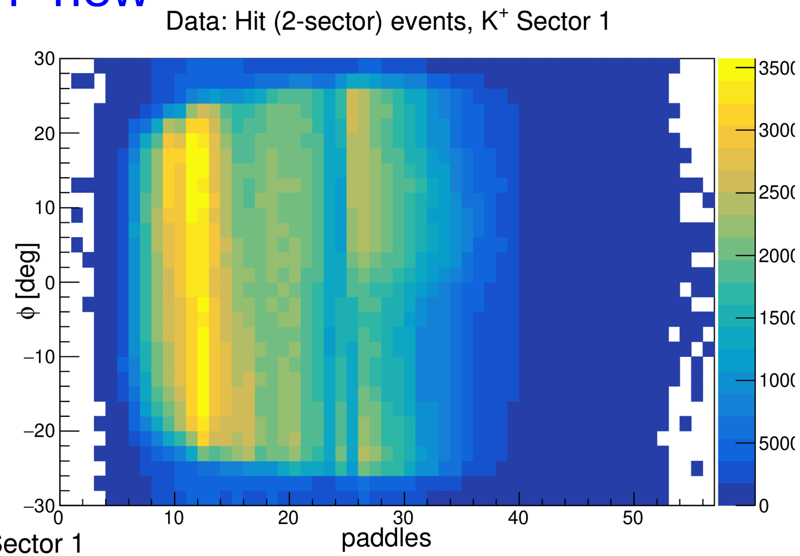

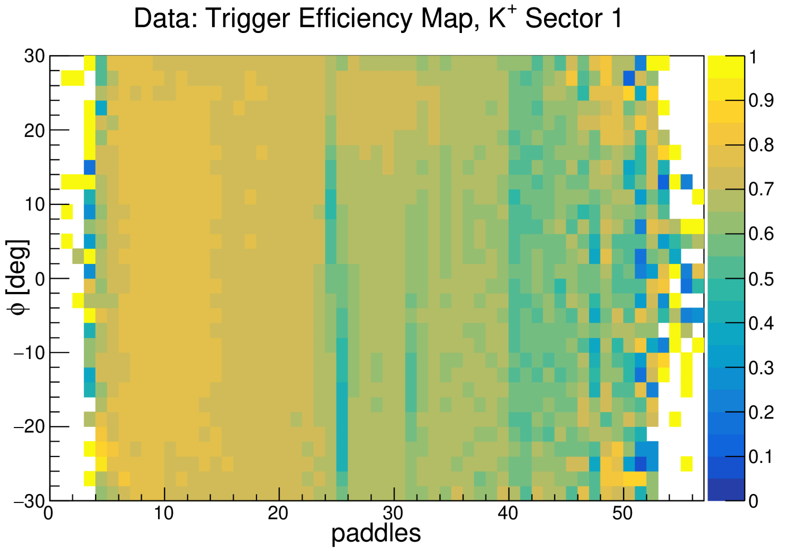

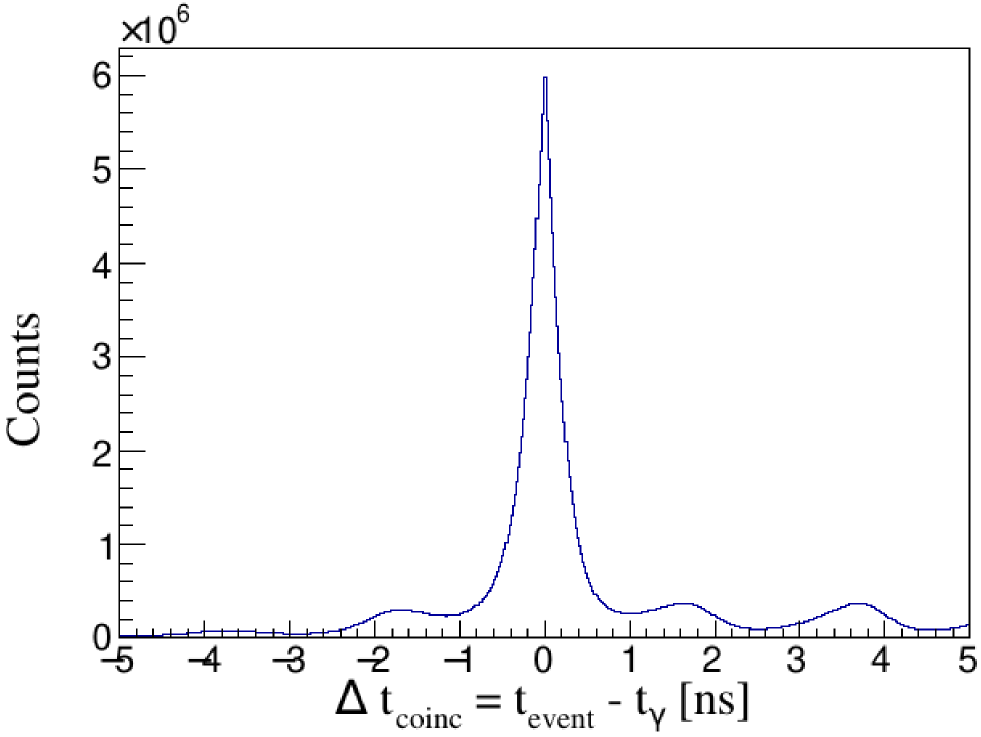

FIG. 2. Shown are the photon coincidence-time distribution, Δt_{coinc}, for the events with K^+, π^+, and π^- as the detected particles. Seen is the 2-ns bunching of the photon beam. Events with $\Delta t_{coinc} = |t_{event} - t_\gamma| < 1$ ns cut on the coincidence-time distribution are selected.

$$\gamma_{corr} = 1 + \frac{N_{N_\gamma>0} - N_{N_\gamma=1}}{N_{N_\gamma>0}}$$

$$\gamma_{corr} = 1.03$$

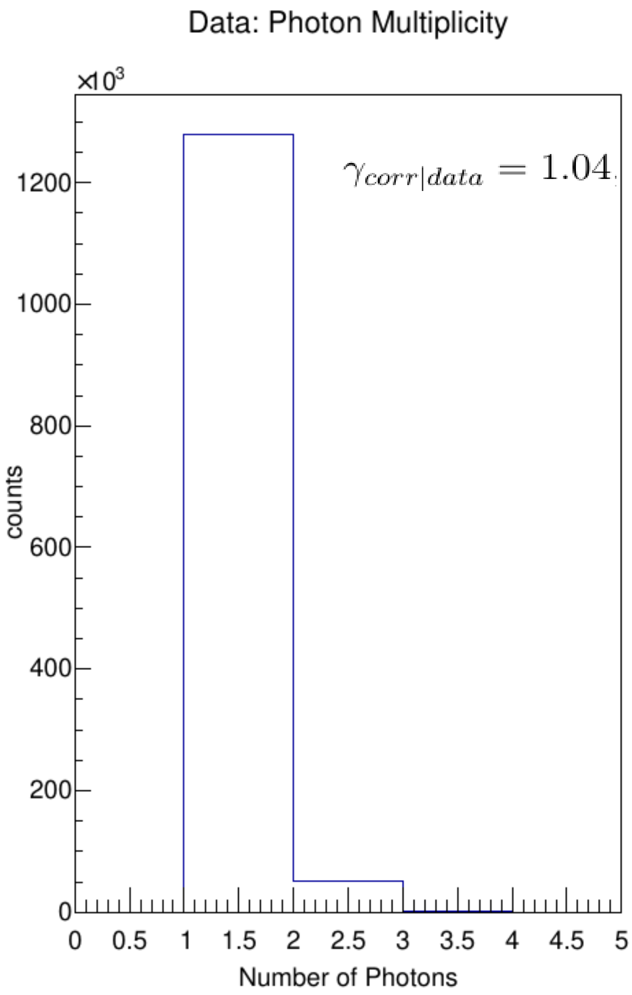

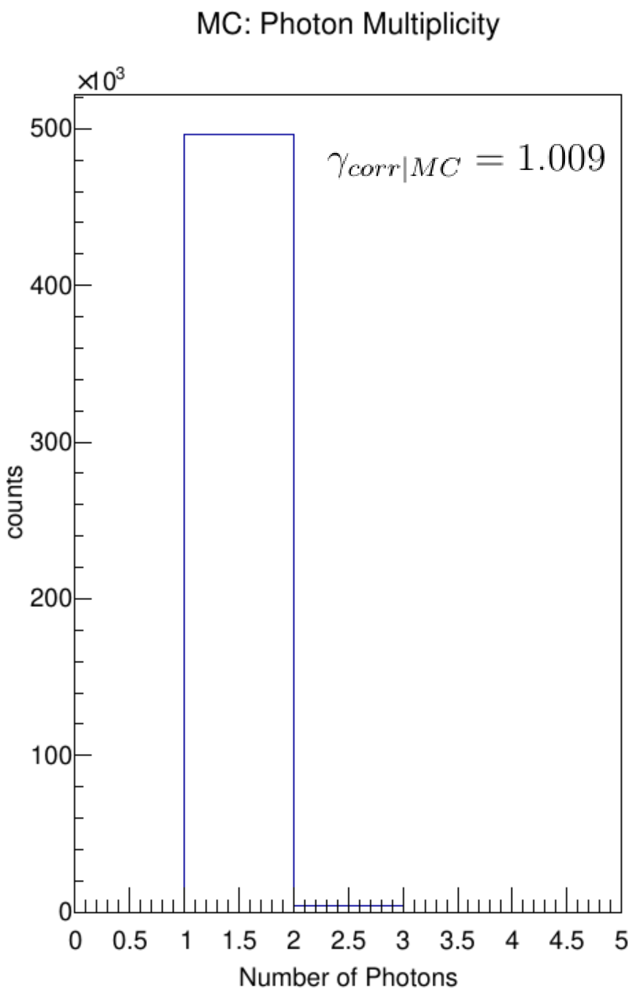

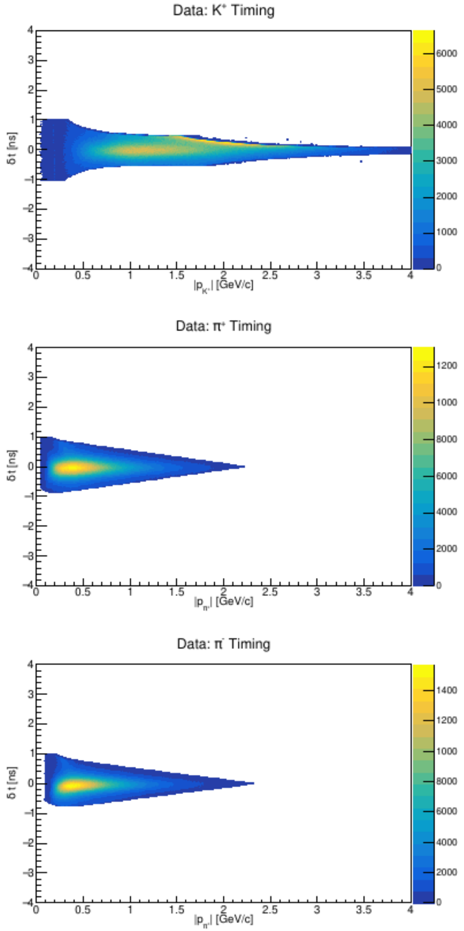

(a) PID plots for Data.

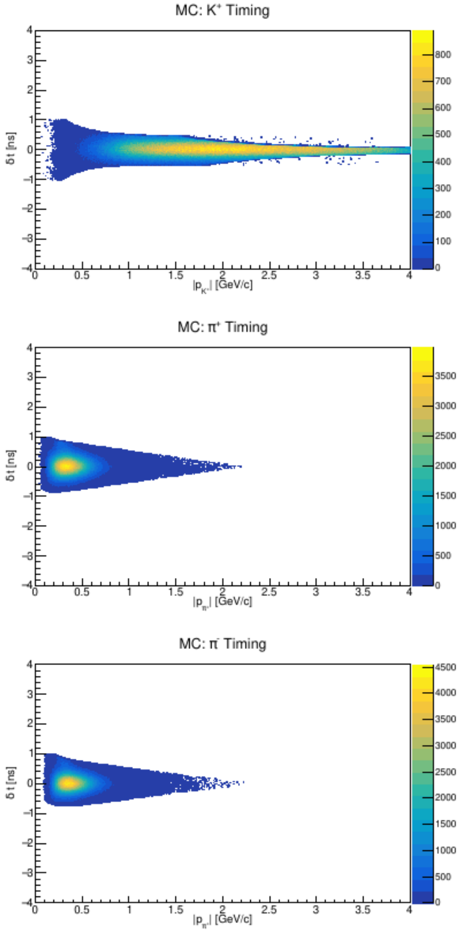

(b) PID plots for MC.

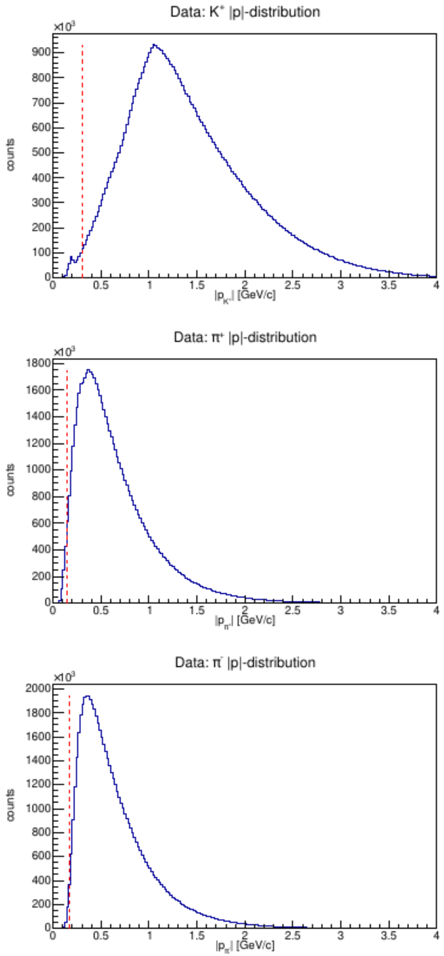

(a) Momentum distributions for the Data.

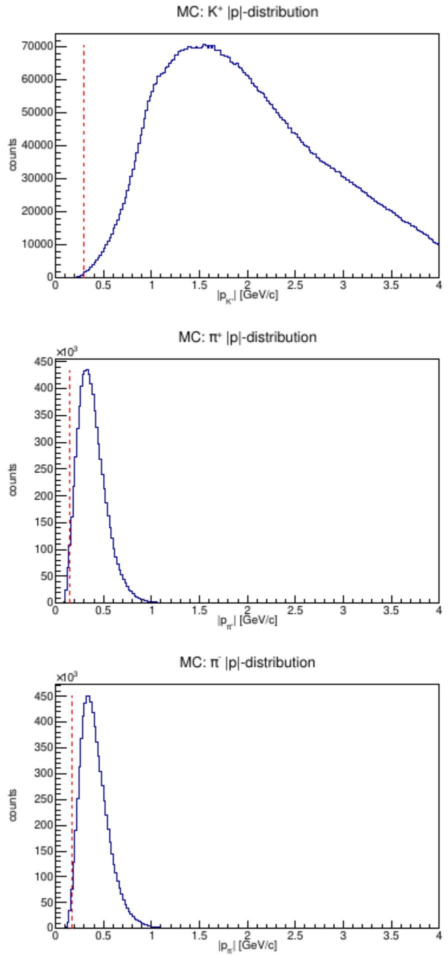

(b) Momentum distributions for the MC.

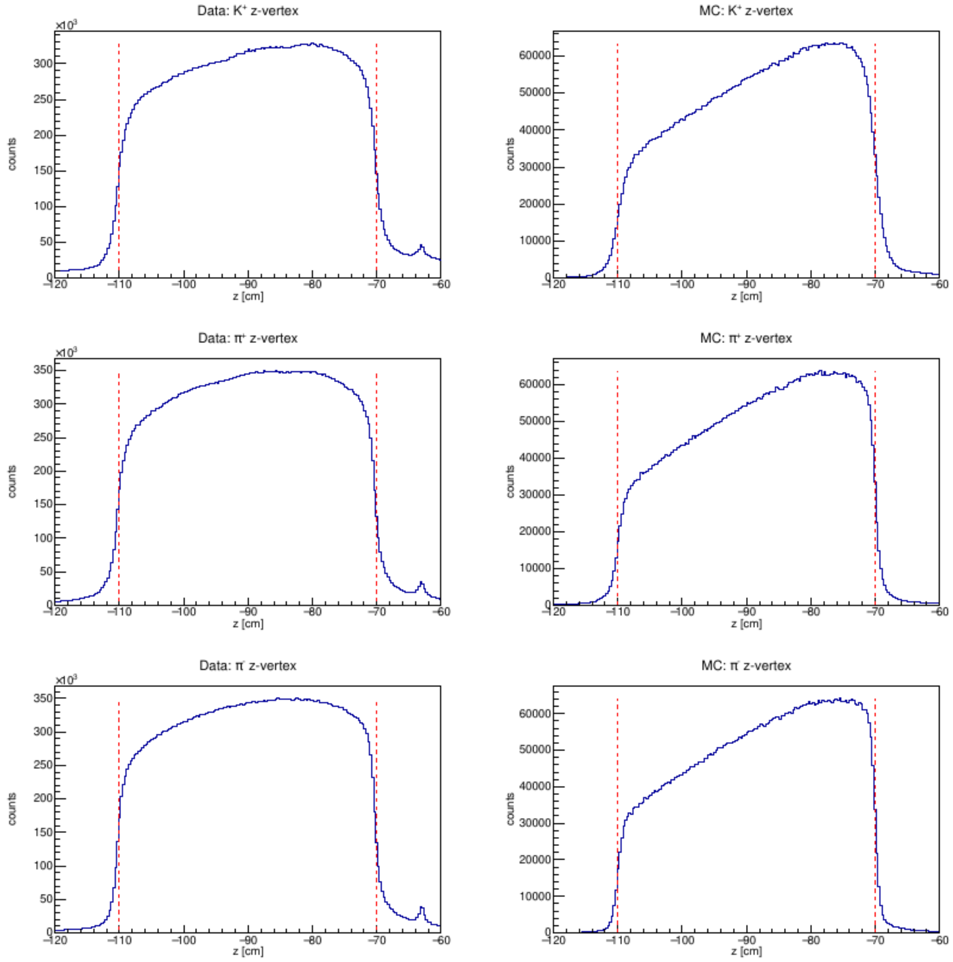

(a) z-vertex distribution for Data.

(b) z-vertex distribution for MC.

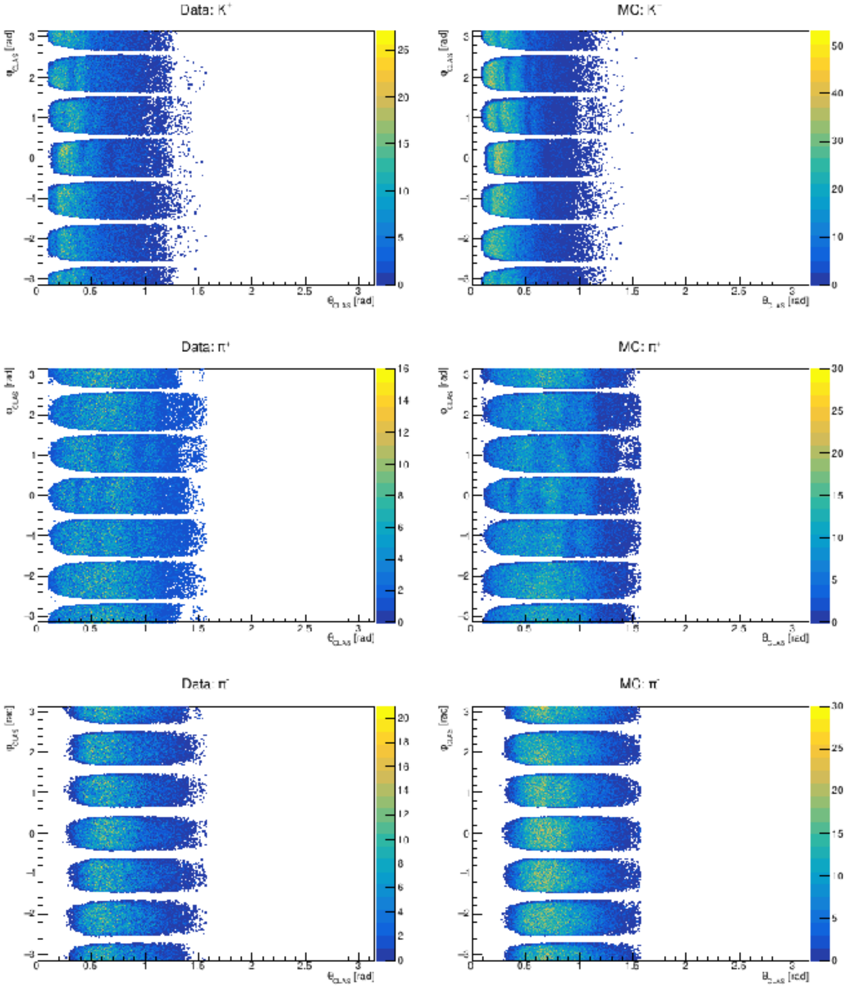

(a) Data: ϕ^{CLAS} vs. θ^{CLAS}.

(b) MC: ϕ^{CLAS} vs. θ^{CLAS}.

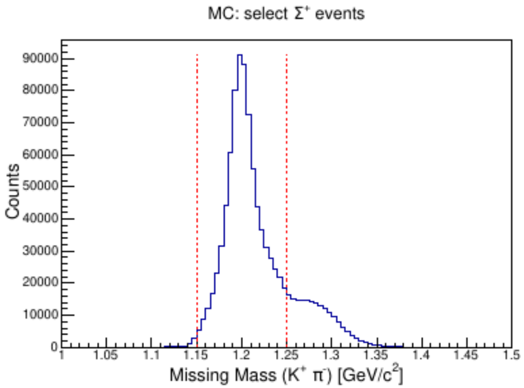

(a) MC: Σ^+ events on $MM(K^+\pi^-)$.

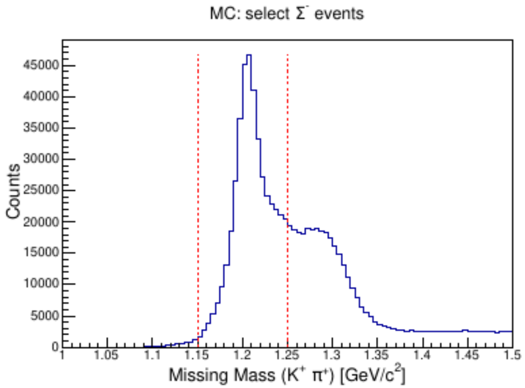

(b) MC: Σ^- events on $MM(K^+\pi^+)$.

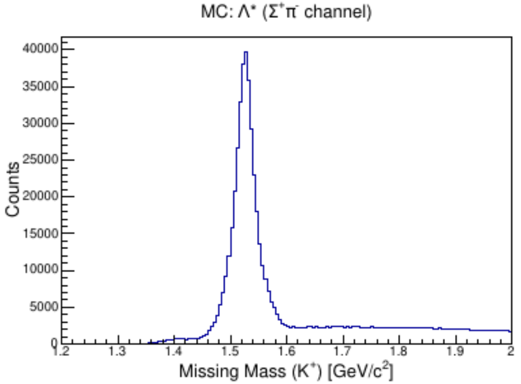

(c) MC: $MM(K^+)$ for Σ^+ cut.

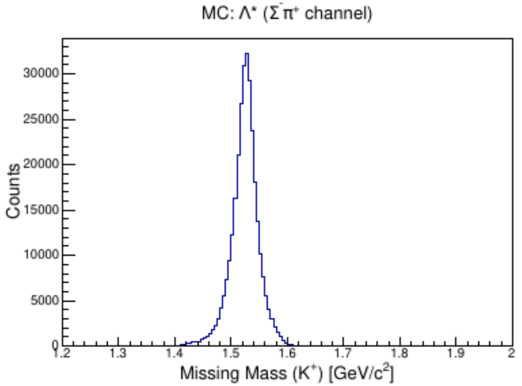

(d) MC: $MM(K^+)$ for Σ^- cut.

Figure 2.19: Missing Mass distributions, showing the $\Sigma^\pm$ peaks and the $\Lambda(1520)$ peaks, when the $\gamma p \to K^{*0}\Sigma^+$ reaction background is added to the usual MC simulations. The added reaction contributes to a flat background to the peaks.

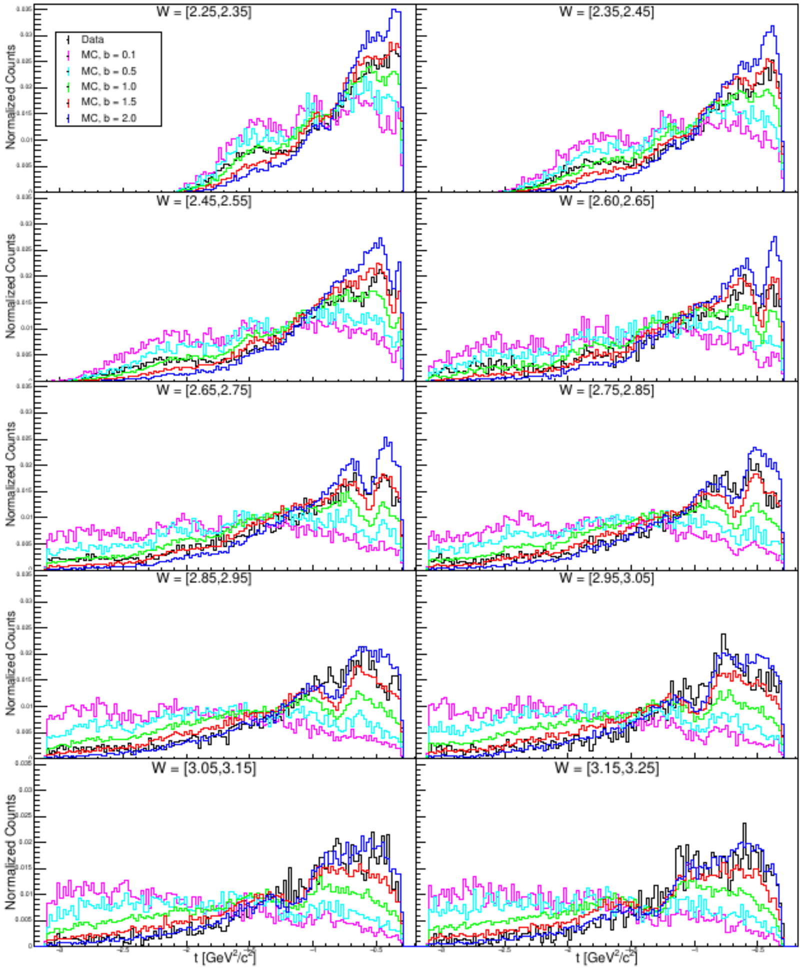

Figure 3.1: Shown are the normalized t-value distribution for the data (black) and simulations with different t-slope parameters, $b = 0.1$ (magenta), 0.5 (cyan), 1.0 (green), 1.5 (red) and 2.0 (blue). The distributions are displayed for increasing W-energy ranges.

$$L(E_W) = \frac{\rho_p N_A l_t}{A_p} N_\gamma(W)$$

$l_t = 40$ cm
$\rho_p = 0.07114\ \mathrm{g/cm^3}$
$A_p = 1.00794$ g/mol
N_A is Avogadro's number

Trigger Efficiency Map